

# blood

2008 111: 4605-4616  
Prepublished online Jan 29, 2008;  
doi:10.1182/blood-2007-10-118844

## Visualization of microtubule growth in living platelets reveals a dynamic marginal band with multiple microtubules

Sunita Patel-Hett, Jennifer L. Richardson, Harald Schulze, Ksenija Drabek, Natasha A. Isaac, Karin Hoffmeister, Ramesh A. Shivdasani, J. Chloë Bulinski, Niels Galjart, John H. Hartwig and Joseph E. Italiano, Jr

---

Updated information and services can be found at:

<http://bloodjournal.hematologylibrary.org/cgi/content/full/111/9/4605>

Articles on similar topics may be found in the following *Blood* collections:

[Hemostasis, Thrombosis, and Vascular Biology](#) (2392 articles)

---

Information about reproducing this article in parts or in its entirety may be found online at:

[http://bloodjournal.hematologylibrary.org/misc/rights.dtl#repub\\_requests](http://bloodjournal.hematologylibrary.org/misc/rights.dtl#repub_requests)

Information about ordering reprints may be found online at:

<http://bloodjournal.hematologylibrary.org/misc/rights.dtl#reprints>

Information about subscriptions and ASH membership may be found online at:

<http://bloodjournal.hematologylibrary.org/subscriptions/index.dtl>



## Visualization of microtubule growth in living platelets reveals a dynamic marginal band with multiple microtubules

Sunita Patel-Hett,<sup>1,2</sup> Jennifer L. Richardson,<sup>1</sup> Harald Schulze,<sup>3,4</sup> Ksenija Drabek,<sup>5</sup> Natasha A. Isaac,<sup>1</sup> Karin Hoffmeister,<sup>1</sup> Ramesh A. Shivdasani,<sup>3</sup> J. Chloë Bulinski,<sup>6</sup> Niels Galjart,<sup>5</sup> John H. Hartwig,<sup>1</sup> and Joseph E. Italiano Jr<sup>1,2</sup>

<sup>1</sup>Translational Medicine Division, Brigham and Women's Hospital, Boston, MA; <sup>2</sup>Vascular Biology Program, Department of Surgery, Children's Hospital, Boston, MA; <sup>3</sup>Department of Medicine, Dana-Farber Cancer Institute and Brigham and Women's Hospital, Boston, MA; <sup>4</sup>Laboratory for Pediatric Molecular Biology, Charité Medical University, Berlin, Germany; <sup>5</sup>Department of Cell Biology and Genetics, Erasmus University, Rotterdam, The Netherlands; and <sup>6</sup>Department of Biological Sciences, Columbia University, New York, NY

**The marginal band of microtubules maintains the discoid shape of resting blood platelets. Although studies of platelet microtubule coil structure conclude that it is composed of a single microtubule, no investigations of its dynamics exist. In contrast to previous studies, permeabilized platelets incubated with GTP-rhodamine-tubulin revealed tubulin incorporation at 7.9 ( $\pm$  1.9) points throughout the coil, and anti-EB1 antibodies stained 8.7 ( $\pm$  2.0) sites, indicative of multiple free microtubules. To pursue this result, we expressed the microtubule plus-end**

**marker EB3-GFP in megakaryocytes and examined its behavior in living platelets released from these cells. Time-lapse microscopy of EB3-GFP in resting platelets revealed multiple assembly sites within the coil and a bidirectional pattern of assembly. Consistent with these findings, tyrosinated tubulin, a marker of newly assembled microtubules, localized to resting platelet microtubule coils. These results suggest that the resting platelet marginal band contains multiple highly dynamic microtubules of mixed polarity. Analysis of microtubule coil diameters in**

**newly formed resting platelets indicates that microtubule coil shrinkage occurs with aging. In addition, activated EB3-GFP-expressing platelets exhibited a dramatic increase in polymerizing microtubules, which travel outward and into filopodia. Thus, the dynamic microtubules associated with the marginal band likely function during both resting and activated platelet states. (Blood. 2008; 111:4605-4616)**

© 2008 by The American Society of Hematology

### Introduction

Platelets are cells that function in maintaining vascular integrity. Their discoid shape enables platelets to travel along the apical endothelium of vessels, where they respond to vascular damage by activating and releasing hemostatic factors. Situated beneath the plasma membrane is a circumferential marginal band composed of 7 to 12 filamentous rings that maintain the discoid shape of resting platelets. Marginal bands assemble in blood cells of other species, but platelets are the only mature human cell possessing a circumferential marginal band.<sup>1</sup>

The platelet marginal band is composed almost entirely of microtubules.<sup>2,3</sup> Microtubules are polymers of  $\alpha\beta$ -tubulin dimers that first associate into linear arrays called protofilaments. Protofilaments laterally associate forming the hollow rigid tubular structure characteristic of microtubules.  $\beta 1$ -Tubulin, a divergent  $\beta$ -tubulin isoform exclusive to megakaryocytes and platelets,<sup>4,5</sup> makes up the bulk of  $\beta$ -tubulin within the microtubule coil.<sup>3,6</sup>

The marginal band preserves the elliptic shape of resting platelets. Transgenic mice lacking  $\beta 1$ -tubulin possess nondiscoid platelets with defective marginal bands containing only 2 to 3 microtubule coils.<sup>7,8</sup>  $\beta 1$ -Tubulin-deficient mice experience thrombocytopenia (platelet counts < 50% of wild-type) and prolonged bleeding times.<sup>8</sup> Chilling of platelets from wild-type mice disassembles their microtubules and induces spherocytosis (spherical

shape). Stabilization of the microtubule coil with paclitaxel prior to chilling prevents spherocytosis and confirms that the microtubule coil is necessary for discoid platelet shape.<sup>9,10</sup>

Platelets are inherently difficult cells to manipulate. They are not amenable to microinjection due to their small size, their lack of a nucleus precludes genetic manipulation, and slight changes in their environment can result in activation. These limitations have prevented direct visualization of cellular dynamics in resting and activated platelets. Insights into cytoskeletal and marginal band structure have come primarily from microscopic analyses. Two distinct models of microtubule organization within marginal bands have emerged from microscopic studies. In the single microtubule model, one continuous microtubule is thought to form the concentric rings of the marginal band. In contrast, the multiple microtubule model holds that several microtubules arranged in either a unipolar or bipolar array form the microtubule coil.

Classic electron microscopy studies of platelet marginal bands completed by Behnke and Zelander in the 1960s,<sup>11,12</sup> White in 1968,<sup>13</sup> Nachmias in 1980,<sup>14</sup> and Kenney and Linck in 1985<sup>3</sup> provide increasingly improved resolution of the microtubule coil and support the single microtubule model. They, however, fall short of providing conclusive evidence that a single microtubule composes the entire coil. Due to the tightly coiled nature of the marginal

Submitted October 18, 2007; accepted January 13, 2008. Prepublished online as *Blood* First Edition paper, January 29, 2008; DOI 10.1182/blood-2007-10-118844.

An Inside *Blood* analysis of this article appears at the front of this issue.

The online version of this article contains a data supplement.

The publication costs of this article were defrayed in part by page charge payment. Therefore, and solely to indicate this fact, this article is hereby marked "advertisement" in accordance with 18 USC section 1734.

© 2008 by The American Society of Hematology

band, which obstructs visualization of individual microtubules, high-resolution images of the coil fail to discriminate between the single microtubule and multiple microtubule models. In addition, in all previous studies, strong fixatives were used to preserve platelets, a method now known to cause the loss of dynamic microtubules.<sup>15</sup> Furthermore, several outstanding questions regarding the platelet marginal band remain unanswered, including (1) how microtubules within the resting platelet marginal band are organized, (2) whether marginal band microtubules are dynamic, and (3) how microtubule reorganization occurs during platelet activation and aging.

In contrast to studies that have established cytoskeletal structure and function within fixed platelets, the studies described here represent the first in which cytoskeletal dynamics have been observed and analyzed in living platelets. Here, novel means were used to examine platelet microtubule coil organization and dynamics. Platelets released from megakaryocytes retrovirally directed to overexpress end-binding protein 3 (EB3) fused to green fluorescent protein (GFP) were examined by time-lapse fluorescent microscopy to observe microtubule remodeling within the marginal band. In addition, we have used incorporation of fluorescent tubulin into the marginal band of permeabilized platelets and immunofluorescence studies with the microtubule end marker, end-binding protein 1 (EB1), to ascertain whether multiple microtubules exist within the marginal band. Antibodies recognizing posttranslationally modified tubulins were also used to examine the accumulation of dynamic and stable microtubules within the coil. Results from these studies contradict the single microtubule model of the marginal band. We observe multiple polymerizing microtubules associated with the marginal band in EB3-GFP-expressing platelets. In addition, we observe incorporation of fluorescent tubulin and localization of EB1 at multiple sites along the marginal band and accumulation of stable and dynamic microtubules in the marginal band. Finally, we show that microtubules within platelets are dynamic during aging and activation. From these data, we favor a model of the marginal band where the coil is composed of multiple, bipolar dynamic microtubules.

## Methods

Approval was obtained from Harvard Medical School and Partner's Human Research Committee for these studies. Informed consent was obtained in accordance with the Declaration of Helsinki. Use of mice in these studies was approved by the IACUC.

### Immunofluorescence of platelets

Mouse or human platelets were purified from whole blood as previously described.<sup>8,16</sup> Mouse platelets were centrifuged onto poly-L-lysine (1  $\mu$ g/mL)-coated coverslips (500g, 2.5 minutes) and fixed in  $-20^{\circ}\text{C}$  methanol with 1 mM EGTA ( $-20^{\circ}\text{C}$ , 10 minutes). Alternatively, platelets were fixed in 4% formaldehyde as previously described and centrifuged onto coated coverslips.<sup>6</sup> For platelet activation, resting platelets were treated with 1 unit/mL human thrombin (Sigma-Aldrich, St Louis, MO; room temperature, 10 minutes) after centrifugation onto poly-L-lysine-coated coverslips, then fixed in either 4% formaldehyde in PBS or  $-20^{\circ}\text{C}$  methanol with 1 mM EGTA. Cells were washed briefly in PBS, permeabilized, and blocked as previously described.<sup>7</sup> Cells were incubated in primary antibody diluted in blocking buffer (10% fetal bovine serum, 1% bovine serum albumin, and 0.05% sodium azide) (room temperature, 1.5 hours or  $4^{\circ}\text{C}$ , overnight) then washed in triplicate with PBS. Antibodies used include 10  $\mu$ g/mL anti-EB1 monoclonal antibody (BD Biosciences, San Jose, CA), 1:100 anti- $\gamma$ -tubulin monoclonal antibody (Sigma-Aldrich), 1:800 anti- $\beta$ 1-

tubulin rabbit polyclonal antibody (gift of Nick Cowan, New York University, New York, NY), and modified tubulin antibodies including 1:500 SuperGlu rabbit antidyrosinated tubulin polyclonal,<sup>17</sup> 1:500 White-wall Tyr rabbit antityrosinated (Tyr) tubulin polyclonal,<sup>18</sup> and 1:500 clone 6-11B-1 mouse monoclonal antiacetylated tubulin (Sigma-Aldrich). Platelets were incubated in secondary antibody conjugated to Alexa Fluor 488 or 568 (Molecular Probes) at a dilution of 1:500 (room temperature, 1.5 hours) followed by 3 washes in PBS. Coverslips were mounted onto microscope slides using Aqua-Mount (Polysciences, Warrington, PA). Fluorescent images of platelets were visualized by fluorescence microscopy using a Nikon Eclipse TE-2000E microscope with 60 $\times$  or 100 $\times$  (NA 1.4) differential interference contrast objectives with a 1.5 $\times$  optivar (Nikon, Melville, NY) and captured with an Orca-II ER cooled CCD camera (Hamamatsu, Hamamatsu City, Japan) equipped with an electronic shutter; shutter and image acquisition were controlled by Metamorph software (Universal Imaging, Molecular Devices, Downingtown, PA). Platelet diameters were measured using the Metamorph software calipers tool.

### Expression of EB3-GFP in platelets

Purified murine megakaryocytes were recovered from single-cell suspensions of murine fetal livers as previously described.<sup>6</sup> Megakaryocytes were infected with EB3-GFP using the pWZL retroviral vector, as previously described.<sup>19,20</sup> Fluorescence microscopy was used to identify infected megakaryocytes based on the expression of GFP. Megakaryocytes cultured for a period of 72 to 96 hours were analyzed for the presence of released platelets, identified by size and presence of a circumferential microtubule band in GFP-expressing cells. EB3-GFP movements were captured by time-lapse fluorescence video microscopy on a Nikon Eclipse TE-2000E microscope using 60 $\times$  or 100 $\times$ /1.4 NA objective lenses and Metamorph imaging software. Cells were maintained at  $37^{\circ}\text{C}$  with a bipolar temperature controller (Medical Systems, Greenville, NY), and images were captured every 2 to 3 seconds with a 200-ms exposure time using an Orca-II ER cooled CCD camera (Hamamatsu).

### Incorporation of rhodamine-tubulin into permeabilized platelets

Resting platelets were permeabilized using 0.4% octyl- $\beta$ -D-glucopyranoside (OG)<sup>16</sup> or 0.5% Triton X-100 in PHEM buffer (60 mM PIPES, 25 mM HEPES, 10 mM EGTA, 2 mM  $\text{MgCl}_2$ ) containing 30  $\mu$ M paclitaxel, 42 nM leupeptin, 10 mM benzamide, and 0.12 mM aprotinin. Permeabilized platelets were incubated in 20 nm rhodamine-labeled tubulin (The Cytoskeleton, Denver, CO) for 4 minutes and 20 nm paclitaxel in PEMG (60 mM PIPES, 10 mM EGTA, 2 mM  $\text{MgCl}_2$ , 0.1 mM GTP) buffer. After incubation, unbound tubulin was removed by washing with PEMG buffer containing 20 nm paclitaxel. Cells were fixed with 3.7% formaldehyde in PHEM buffer for 10 minutes and washed extensively with PHEM buffer. Cells were attached to the surface of poly-L-lysine-coated glass coverslips by centrifugation and visualized by fluorescence microscopy.

### Western blot analysis of platelet lysates

Purified mouse platelets, human platelets, or HEK 293 cells were lysed in SDS-sample buffer containing 2.5%  $\beta$ -mercaptoethanol and immediately heated ( $100^{\circ}\text{C}$  for 5 minutes). Protein concentrations of samples were determined using the RDCD Quantitation kit (Bio-Rad, Hercules, CA). Samples of equal protein load along with a protein ladder (Magic Mark or BenchMark; Invitrogen) were electrophoresed, transferred to membrane, and immunoblotted as previously described.<sup>19</sup> Antibodies to posttranslationally modified tubulins were diluted as follows: Glu (1:1000), anti-Tyr (1:1000) or antiacetylated tubulin (1:1000). Other antibodies used for Western blots included mouse monoclonal anti- $\gamma$ -tubulin (1:1000), anti-EB3 rabbit polyclonal antibody<sup>15</sup> (1:1000), and rabbit anti- $\beta$ 1-tubulin polyclonal antibodies (1:5000). Blots were washed in TBST and incubated in 1:10 000 dilution of HRP-conjugated secondary antibody for 1 hour. Blots were again washed in triplicate in TBST and developed using SuperSignal ECL substrates (Pierce, Rockford, IL). Quantitative analysis of Western blots was performed using Adobe Photoshop software (Adobe Systems, San Jose, CA).

### Induction of thrombocytopenia through treatment with RAMPS or 5-fluorouracil

To obtain a synchronous generation of young platelets, thrombocytopenia was induced in mice using immune depletion with rabbit antimouse platelet serum (RAMPS) or myelosuppression with 5-fluorouracil (5-FU). RAMPS (Inter-Cell Technologies, Jupiter, FL) was diluted 1:100 in sterile saline (0.9% sodium chloride). Mice were intraperitoneally injected with 300 to 500  $\mu$ L diluted RAMPS.<sup>21-23</sup> After a 96-hour recovery period, whole blood was collected from both RAMPS-injected mice and noninjected age-matched control mice through retro-orbital ocular bleeding. Platelets were purified from whole blood by centrifugation.<sup>7</sup> Similarly, mice were injected with 150 mg/kg 5-FU (Sigma-Aldrich).<sup>21-23</sup> After a 10-day recovery period, blood was collected from 5-FU-treated mice and noninjected age-matched control mice through retro-orbital ocular bleeding and platelets were purified.<sup>7</sup> Purified platelets were fixed and processed for immunofluorescence as described above.  $\beta$ 1-Tubulin antibodies were used for immunofluorescence labeling of microtubule coils, whose diameters were measured using the Metamorph Software calipers tool. Comparison of platelet size of control and RAMPS-treated mice was analyzed by flow cytometry (FACS-calibur Flow Cytometer; Becton Dickinson Biosciences, San Jose, CA). After retro-orbital ocular bleeding, whole blood from control mice and RAMPS-treated mice (96 hours after RAMPS infusion) was centrifuged (100g, 8 minutes) to obtain platelet-rich plasma (PRP). PRP from each sample was analyzed by flow cytometry at 10 000 events per sample.

### Paclitaxel treatment of platelets

Platelet-rich plasma (PRP) from human whole blood was purified by centrifugation as previously described.<sup>24</sup> Paclitaxel diluted in platelet buffer was added to PRP to a final concentration of 1  $\mu$ M. Control samples consisted of PRP to which no paclitaxel was added. Samples were either immediately centrifuged onto coverslips and processed for tubulin immunofluorescence as described above, or incubated for 72 hours at room temperature on a platform shaker. After the 72-hour incubation period, the PRP samples were centrifuged onto coverslips and processed for tubulin immunofluorescence. The stained platelets were examined using a Zeiss Axiovert 200M microscope with a 63 $\times$ /1.4 NA objective lens (Carl Zeiss, Heidelberg, Germany). Platelet diameters were measured using the Metamorph software calipers tool. Western blot analysis of paclitaxel-treated PRP and control PRP using  $\alpha$ - and  $\beta$ -tubulin monoclonal antibodies (Sigma-Aldrich) was performed to measure tubulin polymer levels.

## Results

### The platelet marginal band is composed of multiple microtubules

We hypothesize that the platelet marginal band is composed of either a single microtubule or multiple microtubules bundled into a coil. To discriminate between these possibilities we used EB1, a protein implicated in the regulation of microtubule assembly and disassembly,<sup>25-28</sup> as a marker to highlight plus ends of polymerizing microtubules. The single microtubule model predicts that the marginal band will contain one EB1 signal, whereas the multiple microtubule model predicts multiple signals. Anti-EB1 staining of cells in immunofluorescence studies depicts EB1 on a growing microtubule plus end as comets, brightest at their fronts with progressively dimming tails.<sup>29</sup> EB1 comets appeared at numerous points along the microtubule coil of resting platelets (Figure 1A), indicating that several polymerizing microtubules are incorporated into the microtubule coil. Quantitative analysis of platelets labeled with anti-EB1 indicates that on average 8.6 ( $\pm$  2.1) comets occur along each marginal band. The staining pattern of anti-EB1 at distinct points along the microtubule coil clearly differs from that of antitubulin, which continuously labels the entire length of the microtubule coil (data not shown).

To further quantify microtubules associated with the platelet marginal band, we used a second method to identify microtubule assembly sites. We examined the incorporation of fluorescent tubulin within the marginal bands of permeabilized platelets. A microtubule coil consisting of a single microtubule should possess a single plus end. Thus, a single signal should result from the incorporated fluorescent tubulin. However, if the coil encompasses more than one microtubule, multiple signals of incorporated fluorescent tubulin should appear along the periphery of the platelet. Platelets were permeabilized with 0.4% OG, which imparts small holes in the platelet plasma membrane.<sup>16</sup> Previous studies show that lower OG concentrations (0.35%) failed to permeabilize the platelet plasma membrane, while higher concentrations (0.45%-0.5%) eroded large regions of the membrane or removed it entirely.<sup>16</sup> After permeabilization, platelets were incubated in 5  $\mu$ M rhodamine-labeled tubulin for 5 minutes at 37°C. Under these conditions, tubulin approaches its critical concentration and self-nucleation will not occur.<sup>30</sup> Instead, assembly occurs preferentially from the microtubule plus ends. Following incubation, free microtubules and dimers of fluorescent tubulin were removed by washing, and the incorporated tubulin was stabilized with paclitaxel treatment. Fluorescent tubulin incorporated at multiple foci along the periphery of the platelet, suggesting that multiple plus ends reside within the microtubule coil (Figure 2A). On average, 7.93 ( $\pm$  1.9) sites (median = 8 sites, Figure 2B) of incorporated rhodamine-tubulin occurred around the marginal band. In several previous microscopy studies, platelets were permeabilized with Triton X-100 rather than OG prior to examination of the microtubule coil. Triton X-100 treatment results in greater extraction of the plasma membrane than observed with OG.<sup>16</sup> Permeabilization with 0.5% Triton X-100 rather than 0.4% OG altered the pattern of tubulin incorporation. Fluorescent tubulin integrated at a single site on the platelet microtubule coil (Figure 2C), consistent with the presence of a single microtubule. This pattern differs from OG-permeabilized platelets where multiple sites of fluorescent tubulin incorporation were observed (compare Figure 2A and 2C). These results suggest that a higher degree of permeabilization results in the loss of several marginal band-associated microtubules while leaving a single prominent marginal band microtubule intact.

### The platelet marginal band microtubules are dynamic and of opposing polarity

To further test the hypothesis that the marginal band of resting platelets contains multiple microtubules, we examined platelets from megakaryocytes expressing EB3-GFP, an unequivocal marker of polymerizing microtubules. EB3 binds to the microtubule plus end. Previous studies have examined and validated the use of microtubule plus end-associated proteins fused to GFP as a marker for growing microtubules in a number of cell types.<sup>15,19,29,31,32</sup> When bound to polymerizing microtubules, EB3-GFP appears as a comet that tracks with bright fluorescence at its front that gradually dims.<sup>15,29</sup> Megakaryocytes overexpressing EB3-GFP were cultured until platelets were released.<sup>33</sup> Using fluorescence microscopy, we visualized the dynamics of EB3-GFP within platelets. We observed multiple comets, including several that traveled along the microtubule coil in EB3-GFP-expressing platelets, indicating that multiple polymerizing microtubules are associated with the marginal band (Figure 3A; Video S1, available on the *Blood* website; see the Supplemental Materials link at the top of the online article).

We also used EB3-GFP labeling to determine whether microtubules within the marginal band are organized into either unidirectional or bidirectional arrays. The unidirectional model predicts that EB3-GFP comets should move in one direction around the microtubule coil, whereas the bidirectional model predicts the occurrence of both

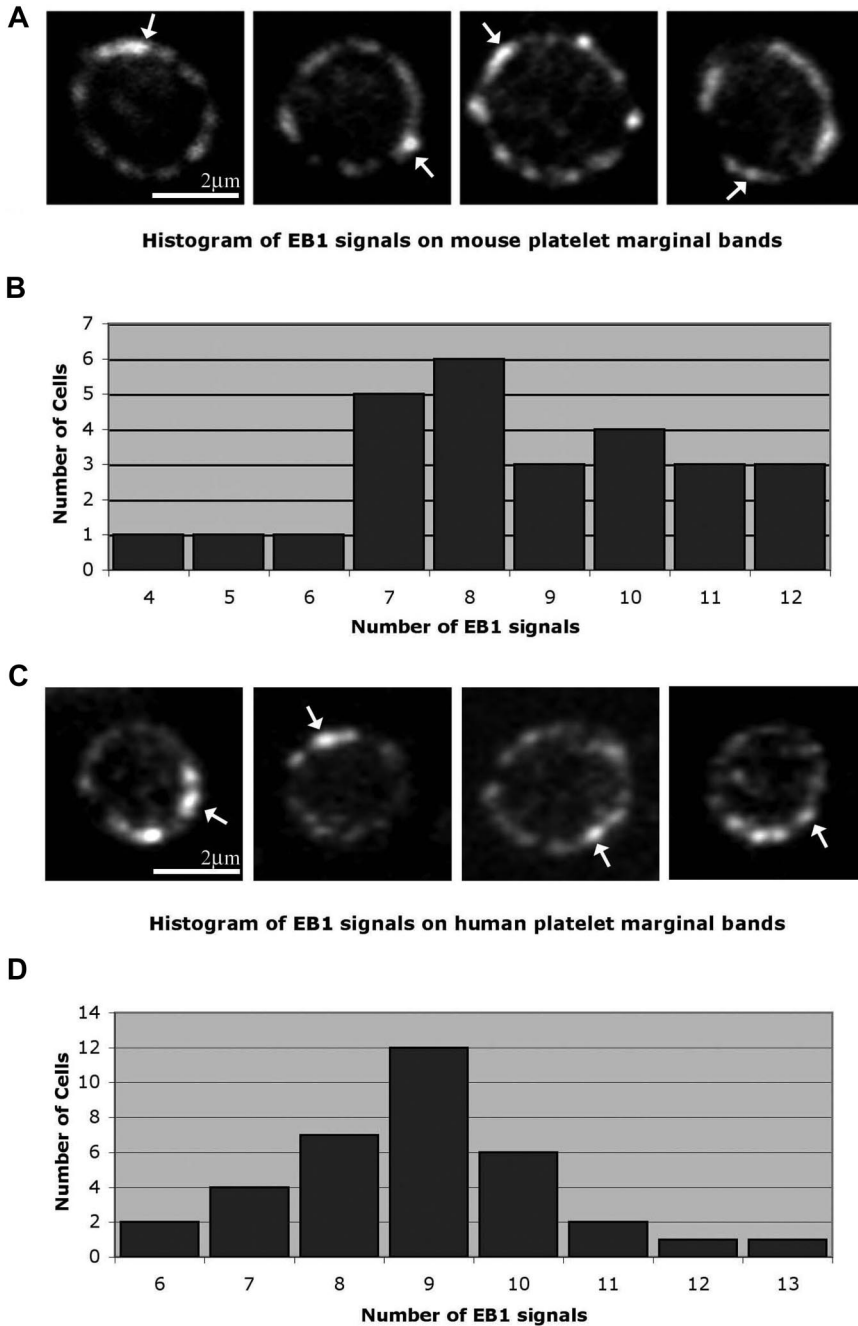


**Figure 1. Localization of microtubule plus ends in the platelet marginal band.** (A) Methanol-fixed resting mouse platelets labeled with anti-EB1 antibodies. EB1 "comets" (→) are labeled along the marginal band. An average of  $8.66 (\pm 2.11; n = 26)$  comets were observed along the marginal band. (B) Histogram showing EB1 signals observed along the microtubule coil of each mouse platelet. The number of signals ranged from 4 to 12, with a median of 8. (C) Anti-EB1 staining in resting human platelets. EB1 comets (→) are identified. An average of  $8.9 (\pm 1.5; n = 34)$  comets are seen along each coil. (D) Histogram of EB1 signals along the microtubule coil of human platelets. The number of signals ranged from 6 to 13, with a median of 9.

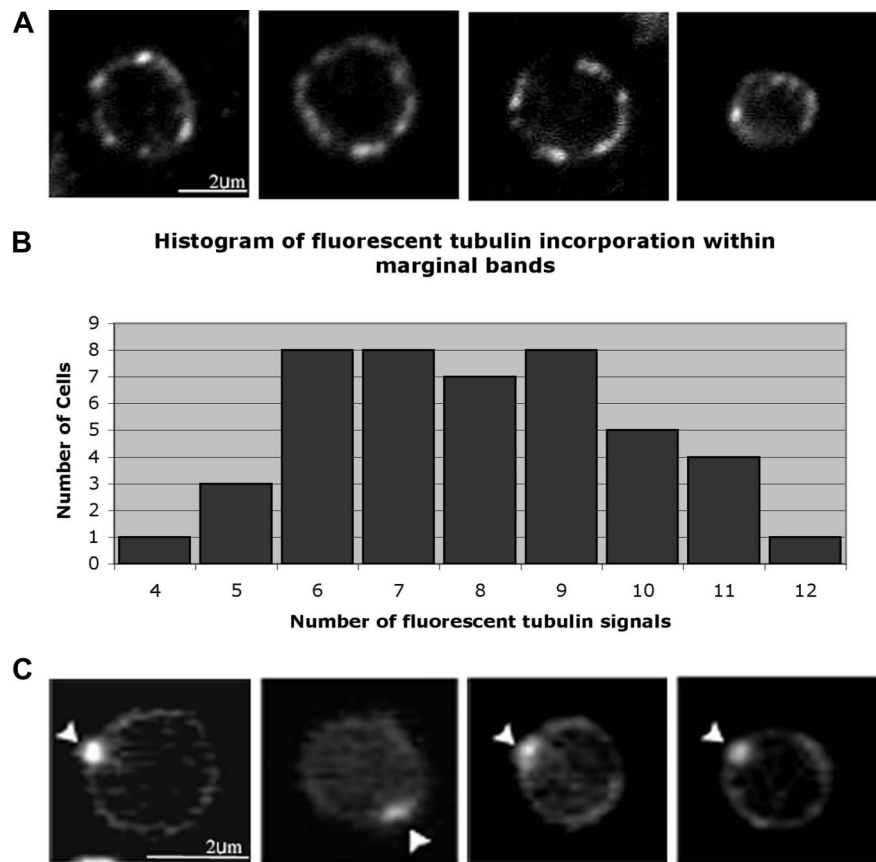
clockwise and counterclockwise movement of cometlike dashes. EB3-GFP comets simultaneously move around the microtubule coil in both clockwise and counterclockwise directions (Figure 3A). Since microtubules traveled in opposing directions, marginal band microtubules must be organized in a bipolar array. The average rate of movement of EB3-GFP within released platelets was  $7.7 (\pm 3.1) \mu\text{m}/\text{min}$ , with a range of  $2.4 \mu\text{m}/\text{min}$  to  $12.2 \mu\text{m}/\text{min}$ . On average, 5 comets were observed traveling the circumference of platelets. Life history plots tracking distance traveled over time of individual EB3-GFP comets within a resting platelet demonstrate that individual microtubules experience variability in growth rates (Figure 3B). In addition to EB3-GFP comets that track along the marginal band, we observed comet movements that appeared to be uncoupled from the marginal band (Video S1). Multiple EB3-GFP comets moved within the interior of the platelet, and we occasionally observed EB3-GFP comets that

transiently move outward beyond the marginal band and then return to the microtubule coil. Since EB3 is endogenously expressed in platelets (Figure 3C), expression of EB3-GFP is unlikely to grossly alter microtubule polymerization within the forming platelet marginal band.

#### Stable and dynamic microtubules comprise the platelet microtubule coil

The stability of microtubules is in part reflected by the degree of posttranslational modifications that occur on the tubulin subunits of stabilized microtubules. Removal of the C-terminal tyrosine from  $\alpha$ -tubulin exposes glutamic acid (Glu-tubulin), an indicator of stabilized microtubules with long half-lives ( $> 1$  hour).<sup>34,35</sup> Cells restore the C-terminal tyrosine (Tyr-tubulin) on tubulin subunits via the tubulin tyrosine ligase enzyme. Accordingly, Tyr-tubulin is a

**Figure 2. Localization of rhodamine-tubulin in platelets.** (A) Mouse platelets permeabilized in 0.4% octyl- $\beta$ -D-glucopyranoside (OG) were incubated with rhodamine-labeled tubulin in 0.1 mM GTP, washed, and then formaldehyde-fixed. Rhodamine-labeled tubulin incorporation at multiple points around the marginal band indicates that free microtubule plus ends exist within the microtubule coil. An average of  $7.9 (\pm 1.9; n = 48)$  signals of rhodamine-labeled tubulin were observed along the periphery of each platelet. (B) Histogram of fluorescent tubulin signals along the marginal band. The number of signals ranged from 4 to 12, with a median of 8. (C) Fluorescence micrograph of purified mouse platelets that had been permeabilized in 0.5% Triton X-100, incubated in rhodamine-labeled tubulin, and then washed and fixed in formaldehyde. Under these permeabilization conditions, rhodamine-labeled tubulin incorporation occurred at a single site ( $\blacktriangleright$ ) along the platelet marginal band.



marker for dynamic microtubules with short half-lives of 5 to 10 minutes.<sup>35,36</sup> Acetylation of tubulin is another major posttranslational modification that occurs in stable microtubules<sup>36</sup> and is sufficient to impart stability to microtubules.<sup>37</sup> Thus, tubulin modification states allow us to discriminate between newly polymerized and older, stabilized microtubules. The multiple EB1 and EB3 comets observed in resting platelets suggest that the marginal band should contain newly polymerized microtubules. Through immunofluorescence microscopy, we investigated the degree of microtubule stability by examining the occurrence of Glu-tubulin, acetylated tubulin, and Tyr-tubulin in purified platelets, all 3 of which were identified in microtubule coils (Figure 4A), confirming previous studies.<sup>37</sup> Furthermore, the staining pattern of all 3 tubulin variants was identical to that of  $\beta$ 1-tubulin, which is distributed throughout the microtubule coil. Therefore, both older, static and newer, dynamic microtubules occur within the marginal band. Western blot analysis of platelet lysates confirms the presence of each modified tubulin (Figure 4C). Examination of platelets stained for both Tyr-tubulin and acetylated tubulin reveals that most platelets contain both dynamic and stabilized microtubules, but the abundance of either isoform appears to vary within a given platelet (Figure 4B).

#### Why are platelet marginal band microtubules dynamic?

Blood platelets circulate for an average of 7 to 10 days in humans and 3 to 7 days in mice. While recent studies indicate that intrinsic regulation of apoptosis directs platelet lifespan,<sup>38</sup> platelets experience numerous changes as they age, such as attenuated response to agonists, alterations in membrane integrity and membrane receptor content, and alteration in granule protein content.<sup>39</sup> It has also been suggested that platelets decrease in size as they age.<sup>40-43</sup> We

reasoned that the marginal band may be required to undergo a similar reduction in size and hypothesized that a dynamic marginal band may be required to accommodate these age-related size changes. To test this hypothesis, we first examined microtubule coil diameters to determine whether platelet marginal bands are dynamic as platelets age. A population of newly formed platelets was generated by treating mice with either RAMPS, which clears the existing platelets from the circulation, or 5-fluorouracil (5-FU), a myelosuppressive agent.<sup>21-23</sup> Newly formed platelets are released into circulation approximately 72 hours after RAMPS treatment and approximately 10 days after 5-FU treatment. After a 96-hour recovery period from RAMPS treatment and a 10-day recovery period after 5-FU treatment, newly formed platelets were purified from whole blood. Analysis of microtubule coils immunolabeled with  $\beta$ 1-tubulin antibodies indicates that newly generated platelets isolated from RAMPS-recovered mice have larger microtubule coils than platelets from control mice (Figure 5A). The average microtubule coil diameter of RAMPS-recovered platelets was  $3.5 (\pm 0.5) \mu\text{m}$ , while control platelets had an average coil diameter of  $2.9 (\pm 0.3) \mu\text{m}$  (Figure 5B). These findings are consistent with flow cytometric analyses, which indicate that platelets of RAMPS-treated mice are larger than control (Figure S1). Similarly, newly formed platelets from 5-FU-recovered mice also contained larger microtubule coils than those from control mice. The average coil diameter of 5-FU-recovered platelets was  $3.5 (\pm 0.7)$  compared with an average coil diameter of  $2.9 (\pm 0.4)$  observed in control mice. Microtubule coil sizes of 5-FU-treated mice returned to control levels after an additional 20 days of recovery.

Given these results, we hypothesized that dynamic microtubules may contribute to the process of marginal band reduction. To assess the

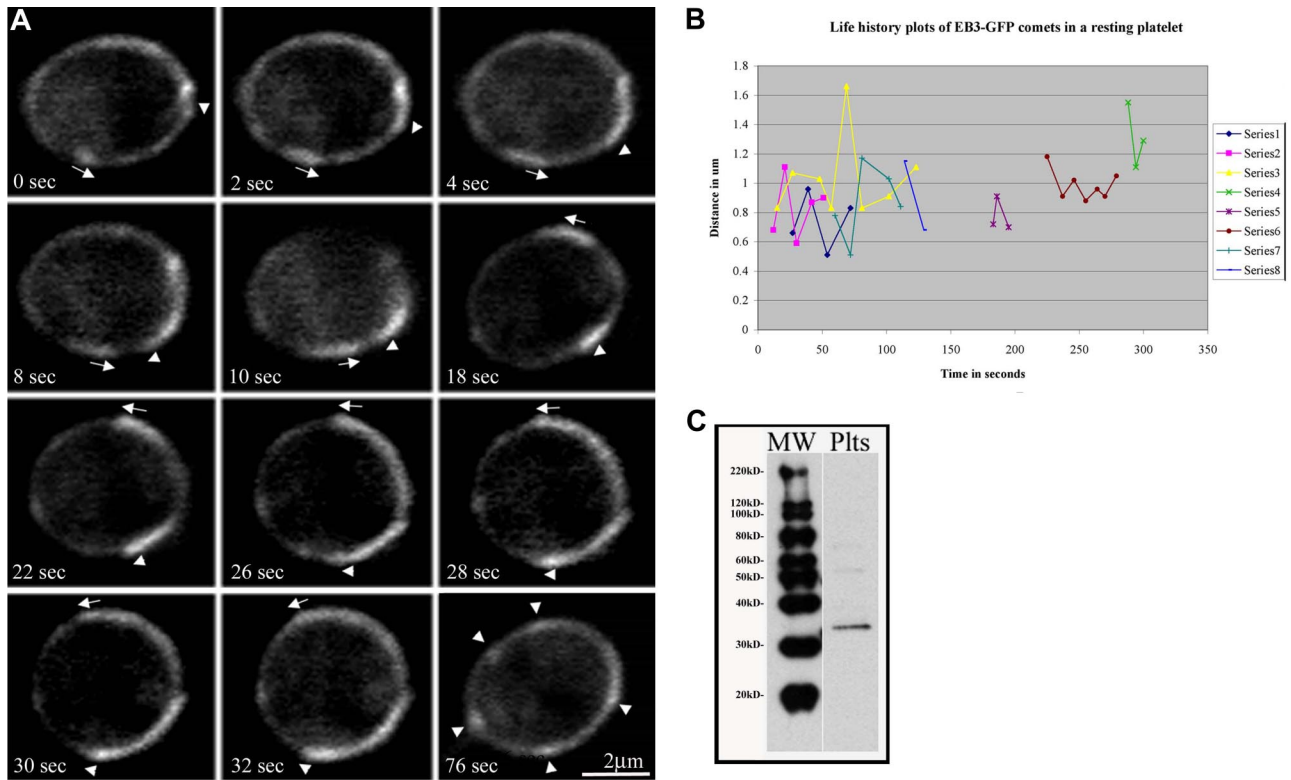


**Figure 3. Multiple microtubules polymerize along the marginal band in living platelets.** (A) Fluorescence microscopy of platelets released from cultured mouse megakaryocytes directed to express EB3-GFP showing the movements of multiple EB3-GFP comets, an indicator of polymerizing microtubules, along the periphery of the platelet. The time course follows a platelet with EB3-GFP comets moving both clockwise (▶) and counterclockwise (←) over the course of 32 seconds. The final panel (76 seconds) shows the same cell with several EB3-GFP comets and foci (▶). (B) Life history plots of 8 individual EB3-GFP comets within a resting platelet show distance traveled over time. (C) Western blot detection of endogenously expressed EB3 in platelet lysates.

role of dynamic microtubules in age-dependent size change, we examined the microtubule coils of human platelets treated with paclitaxel, a drug known to stabilize and inhibit microtubule dynamics. Paclitaxel-treated platelets maintain their original coil size after a 3-day incubation, whereas the microtubule coils of control platelets without drug treatment appear approximately 18% smaller (Figure 5D,E). These results indicate that inhibition of microtubule dynamics prevents age-based platelet size reduction, and supports the premise that dynamic microtubules are necessary for this event.

**Dynamic microtubules polymerize during platelet activation**

Platelets undergo dramatic changes in shape upon activation. Once activated, platelets reorganize their marginal bands, lose their discoid shape, form lamellipodia, and extend filopodia, preparing them for aggregation. We hypothesized that activated platelets undergoing this shape change would possess dynamic microtubules. To examine microtubule polymerization during platelet activation, we performed immunofluorescence studies on activated platelets with anti-EB1 antibodies to

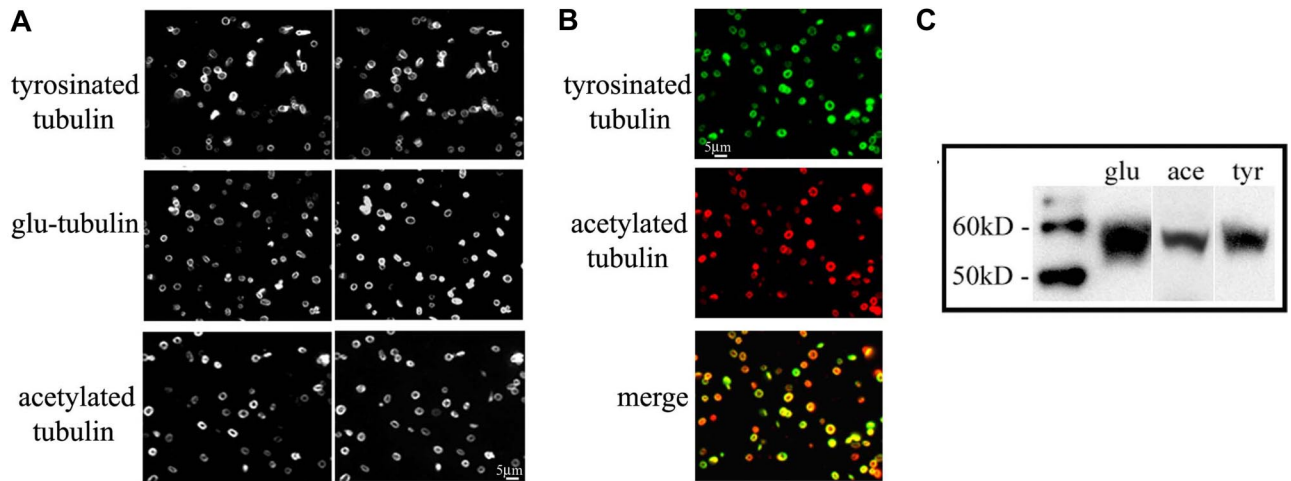


**Figure 4. The microtubule coil contains both stable and dynamic microtubules.** (A) Immunofluorescence analysis of mouse platelets using antibodies to Tyr-tubulin, Glu-tubulin, and acetylated tubulin indicates that all 3 modified tubulin forms exist in the marginal band. Cells were double-labeled with an antibody to  $\beta$ 1-tubulin. (B) Immunofluorescence analysis of mouse platelets using antibodies to Tyr-tubulin (top panel) and acetylated tubulin (middle panel). Note that both isoforms accumulated within platelet marginal bands, although some platelets appear to label more strongly with one antibody than with the other (bottom panel). (C) Western blot of mouse platelet lysates; equal protein quantities were loaded and probed with antibodies to Glu-tubulin (glu), acetylated tubulin (ace), and Tyr-tubulin (tyr).

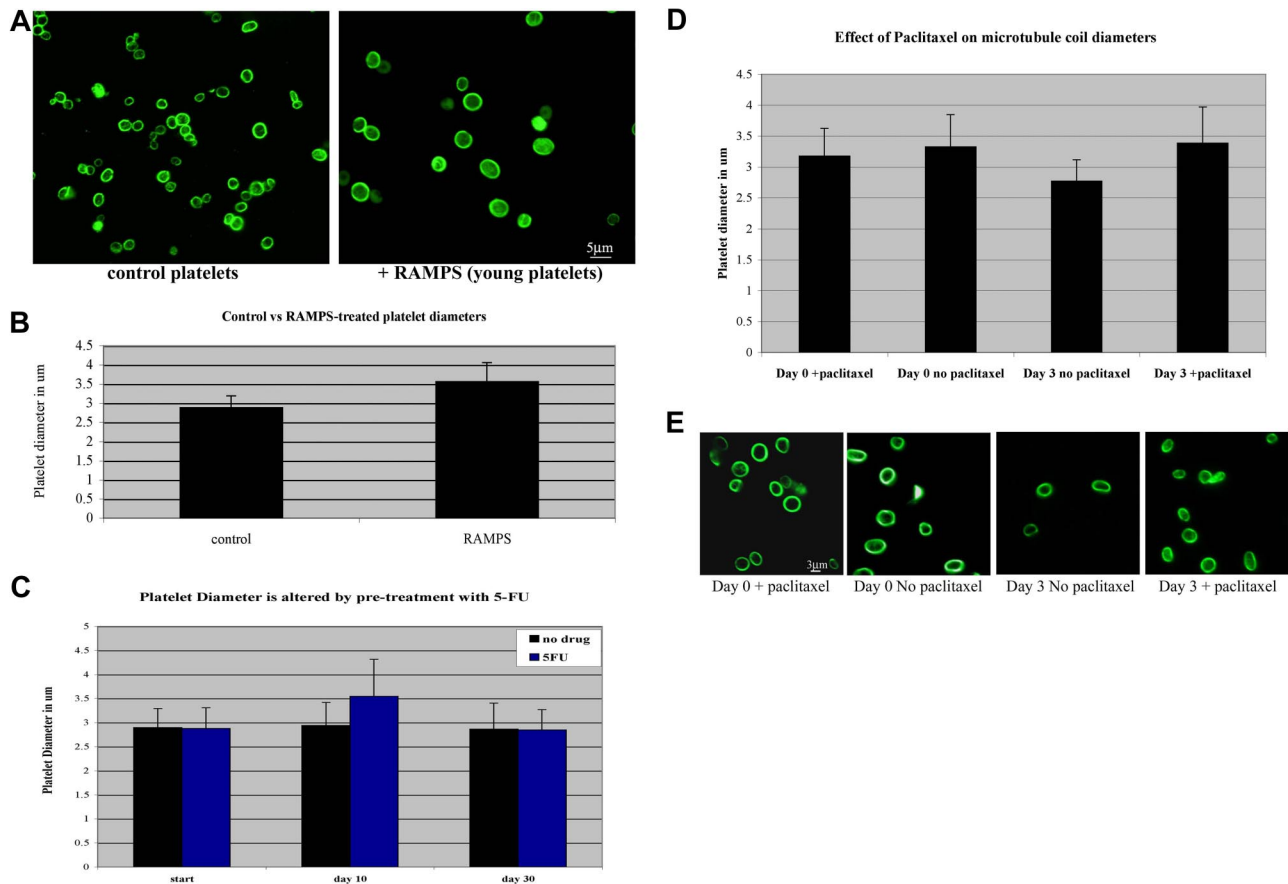


**Figure 5. Microtubule coil diameters decrease in aging platelets and inhibition of microtubule dynamics prevents microtubule coil shrinkage.** (A) Immunofluorescence image of platelets from mice treated with RAMPS (right) and control platelets (left) stained with antibodies to  $\beta$ 1-tubulin show that young platelets have larger microtubule coil diameters than the microtubule coils of normal circulating platelets. (B) RAMPS treatment alters the average platelet diameter. RAMPS-treated platelets averaged  $3.56 \pm 0.5 \mu\text{m}$  ( $n = 31$ ) in diameter, compared with  $2.88 \pm 0.3 \mu\text{m}$  ( $n = 31$ ) for control platelets. Error bars indicate SD. (C) 5-FU treatment alters the average diameter of platelets. 5-FU-treated platelets averaged  $3.54 \pm 0.7 \mu\text{m}$  compared with  $2.94 \pm 0.4 \mu\text{m}$  ( $n = 85$ ) in control platelets. After an additional 20 days, diameters of platelets from 5-FU-treated mice return to control levels. (D) Average microtubule coil diameters of human platelets treated with paclitaxel and nontreated control cells at day 0 and day 3 ( $n = 150$  for each sample). Cells treated with paclitaxel for the 3-day incubation period maintain coil sizes similar to day-0 control cells, whereas day-3 cells incubated without paclitaxel possess smaller microtubule coils. Error bars indicate SD. (E) Immunofluorescence images of human platelets visualized with tubulin antibody labeling. Comparison of day-0 and day-3 platelets plus or minus paclitaxel, as shown, monitors the effect of paclitaxel on the reduction of microtubule coil size.

highlight the plus ends of growing microtubules. EB1 localizes throughout the activated platelets, although it appears more prevalent within lamellipodia and filopodia extended by the cells. Quantification indicates that EB1 localizes to an average of  $25.5 \pm 8.6$ ;  $n = 31$ ) distinct points within a single platelet compared with an average  $8.6 \pm 2.1$  in a resting platelet. Thus, platelets experience a significant increase in microtubule polymerization upon activation. Activated platelets infected with EB3-GFP were examined by time-lapse fluorescence microscopy. The activated EB3-GFP-infected platelets possessed significantly more polymerizing microtubules than resting platelets (Figure 6A; Video S2). Polymerizing microtubules within the activated cell are seen both within the cell and within extended filopodia. The majority of filopodial microtubules (> 90%) consistently appear to polymerize away from the platelet at an average rate of  $3.5 \mu\text{m}/\text{min}$ .

#### A nucleator of microtubules associates with the platelet microtubule coil

The continuous polymerization of microtubules within the marginal band and the increase in microtubule polymerization during platelet activation suggest that platelets, despite lacking a centrosome, contain an element capable of nucleating microtubules.  $\gamma$ -Tubulin, a microtubule nucleator, is required for centrosomal-based nucleation of microtubules.<sup>44</sup> We performed anti- $\gamma$ -tubulin

immunofluorescence in isolated platelets and detected  $\gamma$ -tubulin in distinct foci within the marginal band (Figure 7A,C), a staining pattern similar to EB1. EB1 and  $\gamma$ -tubulin did not colocalize (data not shown), suggesting that  $\gamma$ -tubulin might be localized to the minus ends of microtubules. Quantification of the  $\gamma$ -tubulin labeling within mouse platelets indicates that  $9.06 \pm 1.61$ ; range = 7-12) foci occurred along each microtubule coil. Western blot analysis of platelet lysate confirms the presence of  $\gamma$ -tubulin in platelets (Figure 7E). Thus, although platelets lack centrosomes, they accumulate  $\gamma$ -tubulin, a nucleator of microtubules. Immunofluorescence analysis of activated platelets illustrates that  $\gamma$ -tubulin is primarily restricted to the center of the cell, while microtubules, highlighted by  $\alpha$  $\beta$ -tubulin staining, radiate outward within filopodia (Figure 7F).

## Discussion

Microtubule-based marginal bands confer ellipsoid shapes on certain nucleated invertebrate hematocytes and vertebrate blood cells<sup>45</sup> including blood platelets. Classic electron microscopy studies by Behnke and Zelder,<sup>11,12</sup> White,<sup>13</sup> Nachmias,<sup>14</sup> and Kenney and Linck<sup>3</sup> provided insight into the structure of the microtubule ring in platelets and

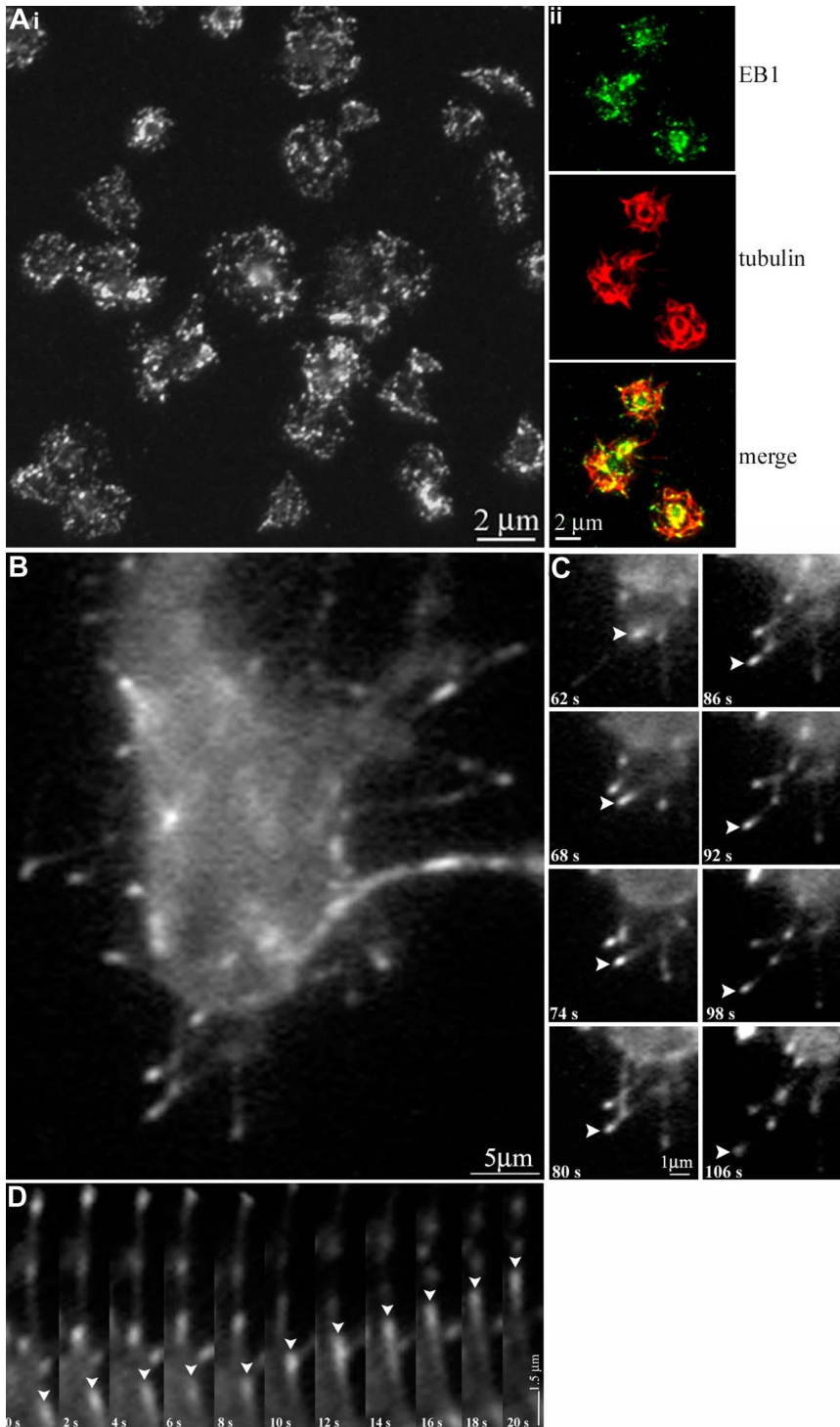


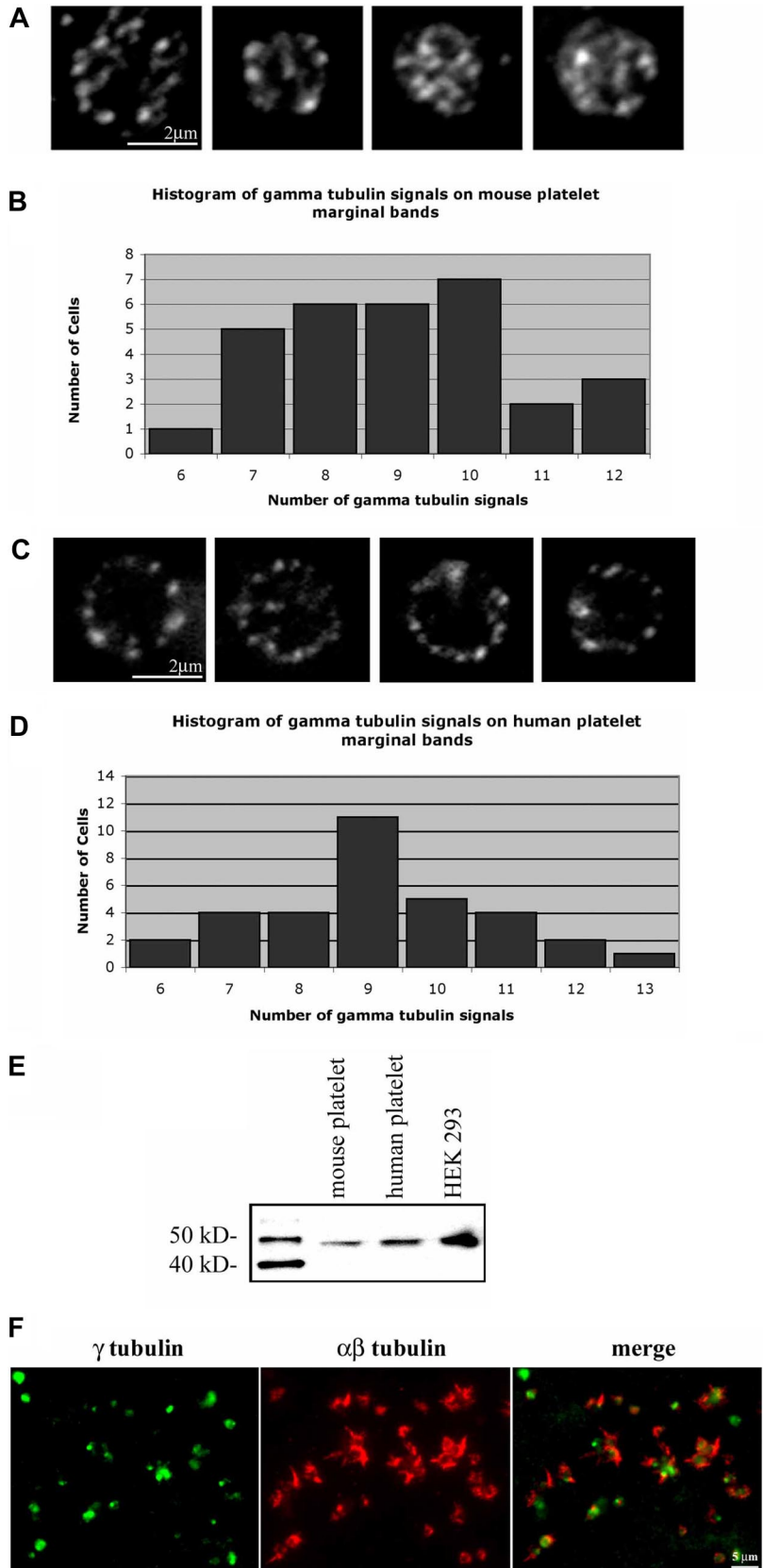
**Figure 6. Visualization of microtubule polymerization in living platelets during activation.** (Ai) Thrombin-activated human platelets fixed and stained with anti-EB1 antibodies. An average of  $25.5 (\pm 8.6)$  sites of EB1 localization are seen. (Aii) Thrombin-activated human platelets fixed and double-labeled with anti-EB1 (green) and antidyrosinated tubulin (red) antibodies. (B) A platelet released from a megakaryocyte infected with EB3-GFP. Note the microtubule growth (indicated by the fluorescent comets) that occurred during activation. (C) In vivo labeling of extended filopodia with multiple EB3-GFP comets. Note (arrowheads) the movement of a single EB3-GFP comet, which appears to move away from the cell body. (D) Kymograph of EB3-GFP comet movements; platelet cell body faces up in this figure. Arrowheads track the movements of a single EB3-GFP comet in consecutive frames.

indicated that it is a coil composed of a single microtubule 100 μm in length. Surprisingly, we find multiple active microtubule plus ends to be associated with the platelet microtubule coil. In particular, we have shown that (1) the plus end assembly protein EB1 localizes at approximately 9 distinct sites on the microtubule coil of mouse and human platelets; (2) fluorescently labeled tubulin incorporates at approximately 9 sites following mild detergent permeabilization of platelets; and (3) multiple microtubules continuously assemble around the periphery of the resting platelet, as determined by time-lapsed video microscopy of EB3-GFP movements in newly released mouse platelets expressing this molecule. Together, these studies provide strong evi-

dence that multiple microtubule plus ends capable of supporting polymerization associate within the platelet marginal microtubule band. The discrepancy between our observations and earlier ones appears to involve the use of Triton-X 100 for permeabilization, as we found that the incorporation of fluorescently labeled tubulin becomes restricted to a single site in platelets that have been extracted with Triton X-100.

In addition to having multiple ends, we find the coil to be dynamic. Platelets expressing EB3-GFP contain multiple microtubules with mixed polarity that polymerize along the marginal band. The average rate of polymerization,  $7.74 \mu\text{m}/\text{min}$ , falls within our previously reported range of microtubule polymerization seen in

**Figure 7. Localization of  $\gamma$ -tubulin in resting and activated platelets.** (A) Purified mouse platelets labeled with anti- $\gamma$ -tubulin antibody show the localization of microtubule minus ends along the microtubule coil.  $\gamma$ -Tubulin foci averaged  $9.06 (\pm 1.61)$  signals along the microtubule coil of each platelet ( $N = 31$ ). (B) Histogram of  $\gamma$ -tubulin signals along the marginal band of mouse platelets. The number of signals ranged from 6 to 12, with a median of 9. (C) Anti- $\gamma$ -tubulin-stained human platelets show localization at multiple points along the microtubule coil. An average of  $9.2 (\pm 1.7; n = 33)$   $\gamma$ -tubulin signals are seen along the coil. (D) Histogram of  $\gamma$ -tubulin signals on the marginal band of human platelets. The number of signals per platelets ranged from 6 to 13, with a median of 9. (E) Western blot detection of  $\gamma$ -tubulin in mouse and human platelet lysates, and HEK 293 cell lysate. Samples of equal protein concentrations were examined. The single protein band detected in each lane shows a relative mobility of approximately 48 kDa, corresponding to the molecular weight of  $\gamma$ -tubulin. (F) Purified human platelets activated with thrombin were formaldehyde-fixed and incubated in anti- $\gamma$ -tubulin antibody (green) and anti- $\alpha\beta$ -tubulin antibody (red). Note the  $\gamma$ -tubulin labeling within the central portion of the activated platelets, while the  $\alpha\beta$ -tubulin extends outward within filopodia.



megakaryocytes. However, the range of rates is broad (2.4-12.2  $\mu\text{m}/\text{min}$ ), suggesting that microtubule movements, such as sliding, may alter the apparent rate of assembly, as seen in proplatelets.<sup>19</sup> Life history plots of individual EB3-GFP comets demonstrate that

dynamic marginal band microtubules experience variability in growth rates. Given an addition rate of 1.6 tubulin subunits per nanometer of microtubule and an average polymerization rate of 7700 nm per minute, approximately 12 300 subunits incorporate

into a single microtubule per minute. With 9 plus ends available for polymerization,  $1.1 \times 10^5$  subunits integrate per minute (1845 subunits/second). Approximately half of the total tubulin content of a resting platelet is in polymer form (31.86 fg per platelet).<sup>46</sup> Thus,  $1.35 \times 10^5$  tubulin subunits remain in the soluble pool, which would be rapidly depleted given the incorporation rate of 1845 subunits/second. Rates of individual growing microtubules did not decrease over time, suggesting that the free tubulin pool is replenished by microtubule depolymerization concurrent with polymerization. This could occur through 2 means: (1) dynamic instability, where the microtubule alternately grows and shortens from its plus end, or (2) treadmilling, where the microtubule shrinks from its minus end as the plus end grows. We favor the mechanism of dynamic instability because EB3-GFP comets are observed only for short periods of time. The fact that we observe EB3 comets for brief periods of time supports dynamic instability rather than treadmilling. That is, treadmilling microtubules will always have a plus end with EB3 bound, while dynamically unstable microtubules have transiently growing plus ends and thus EB3 labeled or unlabeled plus ends.

The hypothesis of constitutive cycling of microtubules in resting platelets finds additional support from the detection of tyrosinated tubulin (Tyr-tubulin) within platelet microtubules. Microtubules containing Tyr-tubulin represent the most recently assembled portion of the polymer. Older, stabilized microtubules (or microtubule portions) are present within the marginal band. Both acetylated and Glu-tubulin isoforms, indicators of stabilized, nondynamic microtubules, localize within platelet marginal bands. Thus, the platelet marginal band has a combination of both dynamic and static microtubules (Figure 8). Based on these findings, we favor a model for the marginal band of the resting platelet that is composed of a single, stabilized prominent microtubule and multiple shorter dynamic microtubules of intermixed polarities. The presence of these additional microtubules changes our view of how the marginal band functions in both the resting and active cell.

#### Platelet microtubules polymerize in response to agonists

Microtubules undergo extensive reorganization following platelet activation. Early in the activation process, the microtubule coil becomes compressed in the cell center. Subsequently, it becomes fragmented or even completely disassembled as individual microtubules appear and grow outward toward the cell periphery. As this reorganization proceeds, we observed a dramatic 3-fold increase in the number of polymerizing microtubule ends, highlighted by EB1 labeling, in thrombin-activated platelets compared with resting platelets ( $25.5 \pm 8.6$  vs  $8.9 \pm 1.5$  EB1 signals in the active and resting cell, respectively). Hence, microtubule nucleation activity is another process controlled by agonist-generated signals. In most cell types, microtubule growth is nucleated by centrosomes. However, since platelets lack centrosomes, it is tempting to postulate that  $\gamma$ -tubulin recruited to the platelet center serves the nucleating function of centrosomes. We further observed that EB3-GFP molecules concentrate at the tips of growing filopodial projections in platelets. Another possible mechanism for generating microtubule plus ends is severing of existing microtubules through the actions of proteins such as katanin or spastin.<sup>47,48</sup>

#### Model of the resting platelet microtubule coil

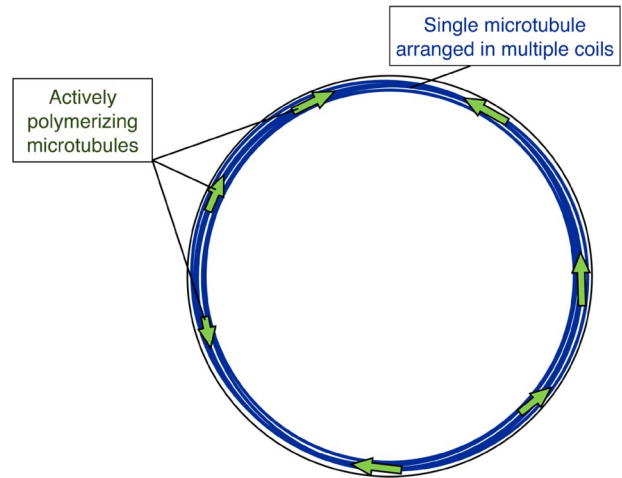


**Figure 8. Model of the resting platelet marginal band.** The model illustrates multiple microtubule coils forming from a single stable microtubule (blue), while several dynamic microtubules (green arrows) polymerize in both directions around the marginal band of the resting platelet.

#### Platelets require dynamic microtubules to accommodate changes in size and shape

In addition to shape changes triggered upon activation, platelets structurally “mature” in circulation.<sup>49</sup> One such maturation event that occurs as platelets age is size reduction. The diameter of the microtubule ring must also diminish accordingly. Coil shrinkage could occur by tightening the coil and/or by recycling the microtubule polymer comprising the coil into the confines of a smaller space. We provided evidence that newly generated platelets (from both RAMPS- and 5-FU-recovered mice) have microtubule coil diameters approximately 15% larger than platelet coils from control mice. Therefore, newly generated platelets possess a mechanism to remodel their microtubule cytoskeleton. Pharmacological inhibition of microtubule dynamics prevents age-related size reduction. Dampening microtubule dynamics with paclitaxel, a microtubule stabilizing agent, has been shown to displace certain plus end-associated proteins involved in dynamics, such as EB1 and EB3, from the microtubule.<sup>50,51</sup> After treatment with paclitaxel, platelet microtubule coils fail to undergo the reduction in size that normally accompanies platelet aging. From this, we conclude that dynamic microtubules are required for marginal band size change.

#### The platelet microtubule coil is a bipolar array

The aim of this study was to discriminate between 2 existing models of marginal band microtubules. These models predict that the microtubules form either a unipolar or bipolar array. In a unipolar array, polymerizing microtubules would move in only one direction around the marginal band. In contrast, polymerizing microtubules would travel in both clockwise and counterclockwise directions around the marginal band in a bipolar arrangement. Analysis of platelets expressing EB3-GFP indicates that microtubules polymerize in both directions around the marginal band. Since growth of microtubules in opposing directions could occur only in a bipolar arrangement, we favor a model of the marginal band in which microtubules occur in a bipolar array with both plus and minus microtubule ends dispersed around the coil.

To conclude, our results support a model in which a principal component of the marginal band is a single, stable microtubule

arranged in a coil. However, unlike previous studies, our results also demonstrate that this microtubule coil associates with multiple, short dynamic microtubules, situated such that a bipolar microtubule array is established within strands of the coil. We have also demonstrated here that these dynamic microtubules are responsible for the platelet's ability to alter its cytoskeleton during physiological processes, such as shrinking its coil during platelet aging, and the formation of a radial microtubule array reaching into forming filopodia during activation and adhesion.

In addition to insights we have made into the dynamics and function of the platelet marginal band, our system of expressing a GFP-linked cytoskeletal protein in a megakaryocyte culture system that produces bona fide platelets represents a novel means of analyzing protein function in living platelets. This approach has enabled us to make the first observations of cytoskeletal dynamics within both resting and activated platelets in real time. Further inquiry into the pharmacological manipulation of microtubule dynamics may lead to development of agents that modify platelet function.

## Acknowledgments

We thank Thomas Stossel and Joseph Loscalzo for providing a supportive laboratory environment; Eva Alden, Giannoula Klement, Robert Flaumenhaft, and Erik Hett for critical review of this paper; and Teresia Magnuson Osborn for providing purified human

platelets. We are also grateful to Dr Judah Folkman for his guidance and support.

S.P.-H. was supported by National Research Service Award fellowship HL082133-01. J.E.I. was supported by National Institutes of Health grant HL068130.

## Authorship

Contribution: S.P.-H. was the primary author of the paper, designed and performed experiments and data analysis, and interpreted results; J.L.R. performed experiments and data analysis, and interpreted results; H.S. and R.A.S. provided reagents and assisted with production of retroviral supernatants and experimental design; K.D. and N.G. provided reagents, performed experiments, interpreted results, and assisted in paper preparation; J.C.B. provided reagents, and assisted with experimental design, interpretation of results, paper preparation, and editing; K.H. and N.A.I. performed experiments, interpreted data, and assisted with paper preparation; J.H.H. designed experiments, interpreted results, and assisted with paper preparation and editing; J.E.I. designed experiments, interpreted results, formulated discussions, and assisted in paper preparation and editing.

Conflict-of-interest disclosure: The authors declare no competing financial interests.

Correspondence: Joseph E. Italiano Jr, Translational Medicine Division, Brigham and Women's Hospital, 1 Blackfan Circle, 6th Floor, Boston, MA 02115; e-mail: [jitaliano@rics.bwh.harvard.edu](mailto:jitaliano@rics.bwh.harvard.edu).

## References

- Behnke O. Microtubules in disk-shaped blood cells. *Int Rev Exp Pathol.* 1970;9:1-92.
- Boyles J, Fox JE, Phillips DR, Stenberg PE. Organization of the cytoskeleton in resting, discoid platelets: preservation of actin filaments by a modified fixation that prevents osmium damage. *J Cell Biol.* 1985;101:1463-1472.
- Kenney DM, Linck RW. The cytoskeleton of unstimulated blood platelets: structure and composition of the isolated marginal microtubular band. *J Cell Sci.* 1985;78:1-22.
- Lewis SA, Gu W, Cowan N. Free intermingling of mammalian Beta-tubulin isotypes among functionally distinct microtubules. *Cell.* 1987;49:539-548.
- Wang D, Villasante A, Lewis S, Cowan N. The mammalian Beta-tubulin repertoire: hematopoietic expression of a novel Beta-tubulin isotype. *J Cell Biol.* 1985;103:1903-1910.
- Lecine P, Italiano JE, Kim S, Villeval J, Shivdasani R. Hematopoietic-specific Beta1 tubulin participates in a pathway of platelet biogenesis dependent on the transcription factor NF-E2. *Blood.* 2000;96:1366-1373.
- Italiano JE, Bergmeister W, Tiwari S, et al. Mechanisms and implications of platelet discoid shape. *Blood.* 2003;101:4789-4796.
- Schwer HP, Lecine P, Tiwari S, Italiano JE, Hartwig J. A lineage-restricted and divergent beta-tubulin isoform is essential for the biogenesis, structure and function of blood platelets. *Curr Biol.* 2001;11:579-589.
- White JG. Influence of taxol on the response of platelets to chilling. *Am J Pathol.* 1982;108:184-195.
- White JG, Rao GH. Microtubule coils versus the surface membrane cytoskeleton in maintenance and restoration of platelet discoid shape. *Am J Pathol.* 1998;152:597-609.
- Behnke O, Zelander T. Substructure in negatively stained microtubules of mammalian blood platelets. *Exp Cell Res.* 1966;43:236-239.
- Behnke O, Zelander T. Filamentous substructure of microtubules of the marginal bundle of mammalian blood platelets. *J Ultrastruct Res.* 1967;19:147-165.
- White JG. The substructure of human platelet microtubules. *Blood.* 1968;32:638-647.
- Nachmias VT. Cytoskeleton of human platelets at rest and after spreading. *J Cell Biol.* 1980;86:795-802.
- Stepanova T, Slemmer J, Hoogenraad CC, et al. Visualization of microtubule growth in cultured neurons via the use of EB3-GFP (End-binding protein 3-Green fluorescent protein). *J Neurosci.* 2003;23:2655-2664.
- Hartwig JH, Bokoch GM, Carpenter CL, et al. Thrombin receptor ligation and activated Rac uncouple actin filament barbed ends through phosphoinositide synthesis in permeabilized human platelets. *Cell.* 1995;82:643-653.
- Bulinski JC, Richards JE, Piperno G. Post-translational modifications of alpha tubulin: deetyrosination and acetylation differentiate populations of interphase microtubules in cultured cells. *J Cell Biol.* 1988;106:1213-1220.
- Gundersen GG, Kalnoski MH, Bulinski JC. Distinct populations of microtubules: tyrosinated and non-tyrosinated alpha tubulin are distributed differently in vivo. *Cell.* 1984;38:779-789.
- Patel SR, Richardson J, Schulze H, et al. Differential roles of microtubule assembly and sliding in proplatelet formation by megakaryocytes. *Blood.* 2005;103:4076-4085.
- Schulze H, Korpai M, Bermeier W, Italiano JE, Walsh SM, Shivdasani RA. Interactions between the megakaryocyte/platelet-specific beta 1 tubulin and the secretory leukocyte protease inhibitor SLPI suggest a role for regulated proteolysis in platelet functions. *Blood.* 2004;104:3949-3957.
- Radley JM, Hodgson GS, Levin J. Platelet production after administration of antiplatelet serum and 5-fluorouracil. *Blood.* 1980;55:164-166.
- Radley JM, Hodgson GS, Thean LE, Zangheri O, Levin J. Increased megakaryocytes in the spleen during rebound thrombocytosis following 5-fluorouracil. *Exp Hematol.* 1980;8:1129-1138.
- Davis RE, Stenberg PE, Levin J, Beckstead JH. Localization of megakaryocytes in normal mice and following administration of platelet antiserum, 5-fluorouracil, or radiostrontium: evidence for the site of platelet production. *Exp Hematol.* 1997;25:638-648.
- Hartwig JH, DeSisto M. The cytoskeleton of the resting human blood platelet: structure of the membrane skeleton and its attachment to actin filaments. *J Cell Biol.* 1991;112:407-425.
- Lansbergen G, Akhmanova A. Microtubule plus end: a hub of cellular activities. *Traffic.* 2006;7:499-507.
- Morrison EE, Wardelworth BN, Askham JM, Markham AF, Meredith DM. EB1, a protein which interacts with the APC tumor suppressor, is associated with the microtubule cytoskeleton throughout the cell cycle. *Oncogene.* 1998;17:3471-3477.
- Rogers SL, Rogers GC, Sharp DJ, Vale RD. Drosophila EB1 is important for proper assembly, dynamics, and positioning of the mitotic spindle. *J Cell Biol.* 2002;158:873-884.
- Morrison EE, Moncur PM, Askham JM. EB1 identifies sites of microtubule polymerization during neurite development. *Brain Res Mol Brain Res.* 2002;98:145-152.
- Ma Y, Sharkiryanova D, Vardya I, Popov S. Quantitative analysis of microtubule transport in growing nerve processes. *Current Biol.* 2004;14:725-730.
- Masuda H, Cande WZ. The role of tubulin polymerization during spindle elongation. *Cell.* 1987;49:193-202.
- Morrison EE. Action and interactions at microtubule ends. *Cell Mol Life Sci.* 2007;64:307-317.
- Akhmanova A, Hoogenraad CC. Microtubule plus-end-tracking proteins: mechanisms and functions. *Curr Opin Cell Biol.* 2005;17:47-54.

33. Italiano JE, Lecine P, Shivdasani R, Hartwig JH. Blood platelets are assembled principally at the ends of proplatelet processes produced by differentiated megakaryocytes. *J Cell Biol.* 1999;147:1299-1312.
34. Webster D, Gundersen GG, Bulinski JC, Borisy GG. Differential turnover of tyrosinated and detyrosinated microtubules. *Proc Natl Acad Sci U S A.* 1987;84:9040-9044.
35. Bulinski JC, Gundersen GG. Stabilization and post-translational modification of microtubules during cellular morphogenesis. *BioEssays.* 1991;13:285-293.
36. Schulze E, Kirschner M. Dynamic and stable populations of microtubules in cells. *J Cell Biol.* 1987;104:277-288.
37. Gundersen GG, Bulinski JC. Microtubule arrays in differentiated cells contain elevated levels of a post-translationally modified form of tubulin. *Eur J Cell Biol.* 1986;42:288-294.
38. Mason KD, Carpinelli MR, Fletcher JI, et al. Programmed anuclear cell death delimits platelet life span. *Cell.* 2007;128:1173-1186.
39. Hartley PS. Platelet senescence and death. *Clin Lab.* 2007;53:157-166.
40. Karpatkin S. Heterogeneity of human platelets: I, metabolic and kinetic evidence suggestive of young and old platelets. *J Clin Invest.* 1969;48:1073-1082.
41. Ginsburg AD, Aster RH. Changes associated with platelet aging. *Thromb Diath Haemorrh.* 1972;27:407-415.
42. Corash L, Shafer B, Perlow M. Whole blood platelet subpopulations: II, use of a subhuman primate model to analyze the relationship between density and platelet age. *Blood.* 1978;52:726-734.
43. Rand M, Greenberg J, Packham M, Mustard J. Density subpopulations of rabbit platelets: size, protein, and sialic acid content, and specific radioactivity changes following labeling with <sup>35</sup>S-sulfate in vivo. *Blood.* 1981;57:741-746.
44. Oakley BR, Akkari YN. Gamma tubulin at ten: progress and prospects. *Cell Struct Funct.* 1999;24:365-372.
45. Lee KG, Braun A, Chaikhoutdinov I, Denobile J, Conrad M, Cohen W. Rapid visualization of microtubules in blood cells and other cell types in marine model organisms. *Biol Bull.* 2002;203:204-206.
46. Steiner M, Ikeda Y. Quantitative assessment of polymerized and depolymerized platelet microtubules. *J Clin Invest.* 1979;63:443-448.
47. Roll-Mecak A, Vale RD. Making more microtubules by severing: a common theme of noncentrosomal microtubule arrays? *J Cell Biol.* 2006;175:849-851.
48. Quarmby L. Cellular Samurai: katanin and the severing of microtubules. *J Cell Sci.* 2000;113:2821-2827.
49. Martin AG, Trowbridge AE, eds. *Platelet Heterogeneity: Biology and Pathology.* London, United Kingdom: Springer-Verlag; 1990.
50. Mimori-Kiyosue Y, Shiina N, Tsukita S. The dynamic behavior of the APC-binding protein EB1 on the distal ends of microtubules. *Curr Biol.* 2000;10:865-868.
51. Perez F, Diamantopoulos GS, Stalder R, Kreis TE. CLIP-170 highlights growing microtubule ends in vivo. *Cell.* 1999;96:517-527.